Minerals Engineering 201 (2023) 108187

Contents lists available at ScienceDirect

Minerals Engineering

journal homepage: www.elsevier.com/locate/mineng

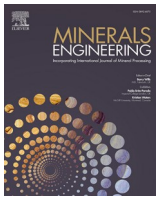

Gravity separation of fine itabirite iron ore using the Reflux Classifier – Part I – Investigation of continuous steady state separations across a wide range of parameters

Armando F.d.V. Rodrigues [a,b], Homero Delboni Junior [b], Otavia M.S. Rodrigues [c], James Zhou [d], Kevin P. Galvin [d,*]

[a] Department of Mineral Processing, Iron Ore, Vale S.A., Brazil
[b] Department of Mining and Petroleum Engineering, Universidade de São Paulo, Brazil
[c] Department of Mining Engineering, Universidade Federal de Ouro Preto, Brazil
[d] ARC Centre of Excellence for Enabling Eco-Efficient Beneficiation of Minerals, Newcastle Institute for Energy and Resources, University of Newcastle, University Drive, Callaghan, NSW 2308, Australia

ARTICLE INFO

Keywords:
Reflux Classifier
Iron ore
Itabirite
Gravity separation
Fluidization

ABSTRACT

High grade iron ore resources are becoming depleted in Brazil, with relatively low-grade ores requiring more intensive concentration to achieve a premium product. Accordingly, a typical industrial itabirite concentration circuit includes desliming in hydrocyclones and concentration via reverse flotation, product thickening and filtration, with the slimes sent to tailings thickeners, and onto tailings storage facilities. This work examined the potential for applying a vastly simpler approach, a single stage of gravity separation using the Reflux Classifier. Here the classified feed, 90 % finer than 0.150 mm, is sent directly to the Reflux Classifier, leading immediately to a high-grade concentrate at high solids concentration.

Part I describes the findings from a comprehensive series of experiments covering the effects of bed density set point, feed pulp density, throughput, fluidisation water rate and lamella channel spacing. The main program, based on an ore with 8 % goethite and 45 % hematite, achieved a feed upgrade from 37 % to 65.6+/−0.4 % iron and iron recovery of 72.9+/−0.4 % at 9 t/m^2/h. A second feed with 1 % goethite and 57 % hematite was upgraded from 41 % to 66.3+/−0.4 % iron at an iron recovery of 84.7+/−0.5 % at 10 t/m^2/h. (The grade of pure hematite is 69.9 % iron). It was essential to run the Reflux Classifier at a sufficient volumetric rate to achieve shear induced inertial lift of the coarse silica within the closely spaced inclined channels, to reject the gangue minerals from the high-grade product. The results demonstrate the technical feasibility of applying the Reflux Classifier to upgrade itabirite feeds.

1. Introduction

The iron and steel industry contributes approximately 8 % of global carbon dioxide emissions (Holappa, 2020). With the growing commitment to achieving net zero emissions of carbon dioxide by the year 2050, there is an imperative to establish a way forward for decarbonizing the industry. A key enabler is the development of more advanced methods of mineral beneficiation to increase the grade of the iron ore (Galvin and Iveson, 2022).

Itabirites, which are typical of the lower grade iron ores, are metamorphic banded-iron formations (Hagemann et al., 2016), consisting of iron oxide (predominantly hematite), with quartz as the main gangue mineral. The processing of the itabirite commences with multi-staged crushing, then grinding, classification and desliming stages, reverse quartz flotation, dewatering of the concentrate, slimes and tailings (Filippov et al., 2014). This conventional circuit requires size distributions finer than 150 μm to achieve adequate liberation (Rodrigues. 2014; França et al., 2020). These flowsheets can upgrade an ore from a typical level of ~ 36 % Fe to 67 % Fe, but are capital intensive (Segura-Salazar et al., 2021) and lead to significant losses of fine iron ore to the tailings due to the need for the desliming.

The performance of the flotation process decreases with increasing particle size due to the tendency for coarse particle detachment in flotation (Dai et al., 2000; Fornasiero and Filippov, 2017; Lima et al.,

* Corresponding author.
E-mail addresses: armando.rodrigues@vale.com, armandodaveiga@gmail.com (A.F.d.V. Rodrigues), kevin.galvin@newcastle.edu.au (K.P. Galvin).

https://doi.org/10.1016/j.mineng.2023.108187
Received 22 February 2023; Received in revised form 29 May 2023; Accepted 12 June 2023
Available online 29 June 2023

2020). The flotation also suffers from losses of ultrafine hematite due to entrainment with the quartz, and from a failure to float ultrafine quartz (Lima et al., 2012. 2016; Filippov et al., 2021) due to the low collision probability between the particles and the bubbles (Fornasiero and Filippov, 2017).

The purpose of the present paper is to examine the potential for applying a much simpler, single stage, gravity separation of the itabirite feed, utilising a Reflux Classifier. Strong performance on fine iron ore has been obtained previously over the size range from 150 μm down to 45 μm using a relatively wide inclined channel spacing of 6 mm (Amariei et al, 2014). The itabirite ore presents a major challenge to gravity separation. Following the grinding, typically 80 % of the particle mass is finer than 150 μm and typically 15–20 % finer than 20 μm. The gravity separation needs to achieve an iron recovery that exceeds the recovery from the reverse flotation circuit at a solids throughput higher than for reverse flotation (typically 4 t/m^2/h), targeting hematite down to about 10 μm. Moreover, the goal is to target a product grade of at least 65 % iron, and ideally up to 68 % iron (pure hematite is 69.9 % iron).

The Reflux Classifier would receive the feed directly from the initial classifier at a pulp density of ~ 26 wt% solids. There would be no need for desliming as required for the preparation of the feed for reverse flotation. This means all the feed is directed to the Reflux Classifier, ideally producing a high-grade concentrate at high solids concentration. This approach offers the potential for removing the desliming cyclones, the reverse flotation, magnetic separators, and the product thickener. There is also no need for flotation chemicals.

The Reflux Classifier consists of a series of inclined channels above an upward current fluidized bed (Galvin, 2021). When the feed enters the system, most of the flow conveys upwards through the system of inclined channels while the faster settling particles segregate downwards towards the lower fluidized bed. Within the inclined channels the denser particles segregate towards the upwards facing inclined surfaces, forming a sediment that slides downwards (Galvin, 2021). Lower density particles experience shear induced lift, exposing those particles to the higher upwards velocities within the inclined channels, conveying those particles upwards. Fluidization water supports the formation of a lower fluidized bed, while also delivering strong desliming. Pressure transducers are used to quantify the suspension density in the lower fluidized bed. The control valve opens when the measured suspension density exceeds the value of the set point.

The inclined channels have a perpendicular spacing, z, which, for a given superficial flow velocity, governs the shear rates within the flow field of the inclined channels, and hence the hydrodynamic lift force that acts on the particles. In previous work conducted primarily on coal, a channel spacing of 6 mm was used, sufficient to deliver the lift force necessary to convey relatively coarse particles of low-density coal upwards through the inclined channels. Amariei et al (2014) used the 6 mm channel spacing for fine iron ore feeds, however the effectiveness was limited to a relatively narrow size range. More recently, with an increasing focus on dense minerals, a channel spacing of z = 3 mm has been used to deliver the much larger lift force necessary to convey relatively coarse particles of silica and other gangue minerals to the overflow, while extending the recovery of the higher density particles in the underflow product to include finer particles.

The present work examines the upgrading of itabirite ores using even more closely spaced channels with z = 1.8 mm. These closely spaced channels should in principle lead to stronger rejection of the coarse silicates while also increasing the capture of the ultrafine hematite below 20 μm. These two benefits should increase the potential for replacing the existing beneficiation circuits described above with a vastly simpler single stage gravity device.

The obvious concern with utilising closely spaced channels is whether there is an increased potential for blockages to develop. It is important to appreciate there is a considerable difference between a planar channel and conduit. The planar channel delivers a critical additional degree of freedom, which allows particles to readily develop trajectories around other particles. Thus, the tendency for blockage is counter-intuitive, indeed exceedingly low. Moreover, the higher shear rates produce a cleaning effect within the channels, preventing any compaction of sediment. In general, the tendency for particle blockage is negligible, though it is appropriate that oversize protections be applied to circuits.

This study provides a comprehensive investigation of the gravity separation of the fine iron ore feed achieved by the Reflux Classifier, covering the effects of changes in the volumetric feed rate, bed density set point, feed pulp density, fluidization velocity, and channel spacing. In a subsequent Part II of this study, these data sets are investigated theoretically, applying a partition surface to a binary hematite-silica representation of the feed as a generalized model to predict the grade and recovery. It is noted the binary components incorporate minor adjustments in their compositions to include features in the mineralogy.

2. Experimental

2.1. Ore samples

Samples from two itabirite mines were collected at industrial plants operated by Vale and located in the Iron Quadrangle of the state of Minas Gerais, Brazil. Fig. 1 shows the point from which a 700 kg Sample A was obtained. In this case, the fines formed naturally through the breakage of the ore to pass ~ 0.15 mm. Sample B was processed further as shown in Fig. 2, using wet grinding of the ore to pass ~ 0.15 mm.

2.2. Feed ore characteristics

Table 1 presents the nominal chemical assays as a function of the particle size showing the relatively low iron grade, less than the richer Brazilian ores. It is also evident the coarser particles are rich in silica and hence the iron concentrates much more in the finer sizes. Table 2 shows the mineralogy, by optical microscopy, the dominant minerals being hematite and quartz. Fig. 3 shows the complete particle size distribution of the two samples including the significant proportion of ultrafine particles below 10 μm. All assays were obtained using XRF. Optical mineralogy was undertaken using a polarization microscope. It is noted these samples were taken as aliquots at the mine prior to the experimental work so are included primarily for illustrative purposes.

2.3. Methodology

A laboratory scale Reflux Classifier, with horizontal cross-section 0.1 m × 0.1 m, vertical height of 1 m, and inclined section containing parallel channels of 1 m is shown in Fig. 4. Fluidization water was distributed through 16 holes, each 0.8 mm in diameter. The experimental program utilised a system of inclined channels with perpendicular spacing of 1.8 mm, with some additional experiments conducted using the wider channel spacing of 3.0 mm. This is the first comprehensive study of a Reflux Classifier operated using a 1.8 mm channel spacing.

The authors have provided a Supplementary Data Source with this paper outlining the approach used to ensure high quality, and accurate data were produced in this study. The Supplementary provides additional data sets and expands on the analysis of the errors described later in the paper. The system adopted for feeding the Reflux Classifier (RC) commenced with a preparation phase. The entire sample was added to a 1300 Litre feed tank, water was added to adjust the pulp density, then the entire sample was discharged into 20 Litre buckets. The buckets were numbered and randomly sorted via a random number generator, and then stacked ahead of the experimental facility as shown in Fig. 5. Then, a much smaller 300 Litre feed tank was used to supply the feed to the Reflux Classifier, the level maintained by adding the random sequence of buckets to the tank. The feed tank operated with a stirrer, a set of baffles, and a circulation flow was generated out of the bottom of

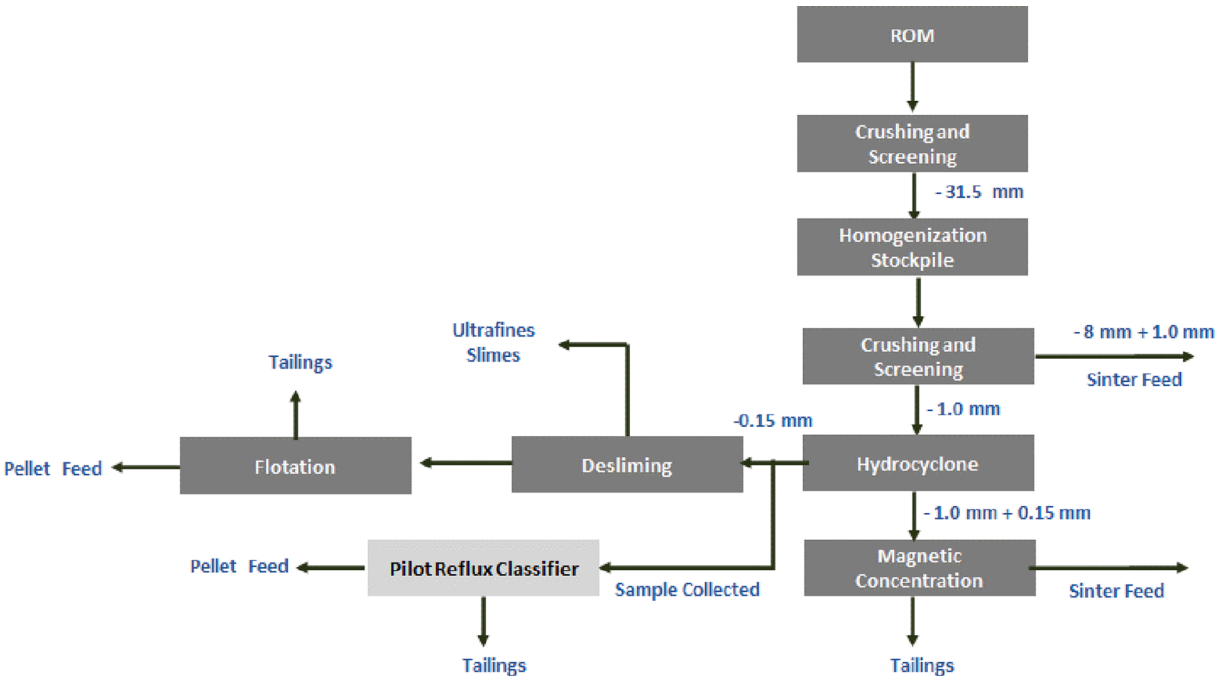

Fig. 1. Industrial itabirite plant sampling point – Sample A.

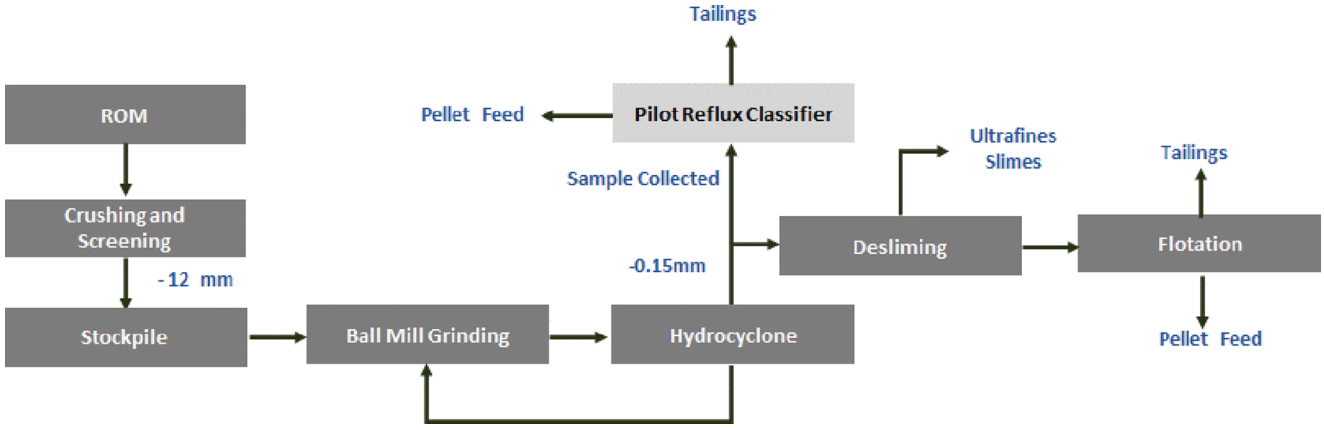

Fig. 2. Industrial itabirite plant sampling point – Sample B.

Table 1
Nominal chemical assays by size.

Size (mm)	Mass (%)	Fe (%)	SiO_2 (%)	P (%)	Al_2O_3 (%)	Mn (%)	LOI (%)
Sample A							
+0.150	12.7	18.9	72.2	0.017	0.26	0.053	0.44
−0.150 + 0.045	53.6	32.2	52.8	0.017	0.31	0.040	0.46
−0.045 + 0	33.8	53.1	18.4	0.072	2.85	0.370	2.43
Overall	100.0	37.3	43.3	0.041	1.31	0.194	1.40
Sample B							
+0.150	14.2	4.5	92.6	0.010	0.28	0.016	0.22
−0.150 + 0.045	38.3	34.0	50.7	0.010	0.22	0.016	0.13
−0.045 + 0	47.5	57.2	17.0	0.011	0.45	0.023	0.24
Overall	100.0	40.9	40.7	0.010	0.34	0.019	0.20

Table 2
Nominal mineralogy.

Hematite (%)	Magnetite (%)	Goethite (%)	Quartz (%)	Manganese Oxides (%)	Gibbsite (%)	Others (%)	Quartz Liberation (%)
Sample A							
45.13	3.09	7.94	43.0	0.28	0.53	0.00	100
Sample B							
56.76	0.00	1.04	41.4	0.02	0.02	0.73	99

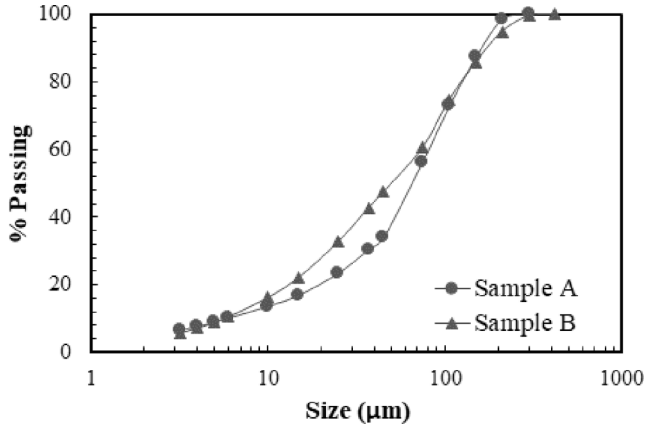

Fig. 3. Nominal particle size distributions of the two samples.

the tank and back into the tank using a centrifugal pump. A peristaltic feed pump operated off this circulation line to supply the feed to the Reflux Classifier.

The method of feed preparation and delivery was successful in maintaining the assays and particle size distribution across a given experiment and across the entire campaign. Steady state samples of the underflow product, and overflow reject were collected simultaneously over the same period, followed by a sample of the feed. These were weighed, dried, and subjected to desliming, and dry sieving. Sample assays were secured from an external commercial laboratory. All data from the experiments were subjected to mass balance reconciliation (Galvin et al, 1995). A Simplex Search Technique, guided by an objective function, was used to optimise the overall material balance. The objective function is formed from the errors generated during the mass balancing, given by the weighted sum of the errors squared. The weighting is given by the inverse of the estimated variance in the experimental value. Based on the analysis of 13 feed samples, sieve analysis is assumed to carry a standard deviation of 10 % of the experimental value while assays are assumed to carry a standard deviation of 1 %. Ultimately it is the internal consistency in the data that matters. This procedure delivered high level agreement between the raw experimental values and the mass balanced data as shown later.

2.4. Laboratory-scale experiments – Sample A, B

The present work offered an opportunity to undertake a systematic approach to traverse the phase space of this system, guided by established fundamental principles. Thus, in most of the experiments undertaken in this study only a single parameter was changed at a time, thus allowing the direct effect of that change to be evaluated. The experimental methodology described in the previous section had the effect of eliminating much of the feed variability that plagues many experiments of this kind (Crompton et al, 2022; Starrett and Galvin, 2023), ensuring the provision of very consistent experimental data. During the experimental campaign, building on the knowledge developed from former experiments, more than one change was introduced at a time into a single experiment to capture multiple benefits. Ultimately, the program of work provided a substantial data set and in turn a direct insight into the complexities of the particle transport in the Reflux Classifier.

The feed used for the main campaign was Sample A, reconstituted at the end of each experiment. Table 3 summarizes the conditions applied. For example, the first three experiments involved volumetric feed flow rates of 2, 6, and 4 Litres per minute. The channel spacing was 1.8 mm, the density set point 2000 kg/m^3, feed pulp density 26 %, and fluidization rate 0.14 L/min (except for Run 1 which used 0.12 L/min). The nominal solids throughputs are listed showing a range from 5 to 14 t/m^2/h.

In the following three experiments the density set point was varied, covering 1900, 2100, and 2200 kg/m^3, while the feed flow rate was fixed at 5 L/min. Again, the channel spacing was fixed at 1.8 mm, the

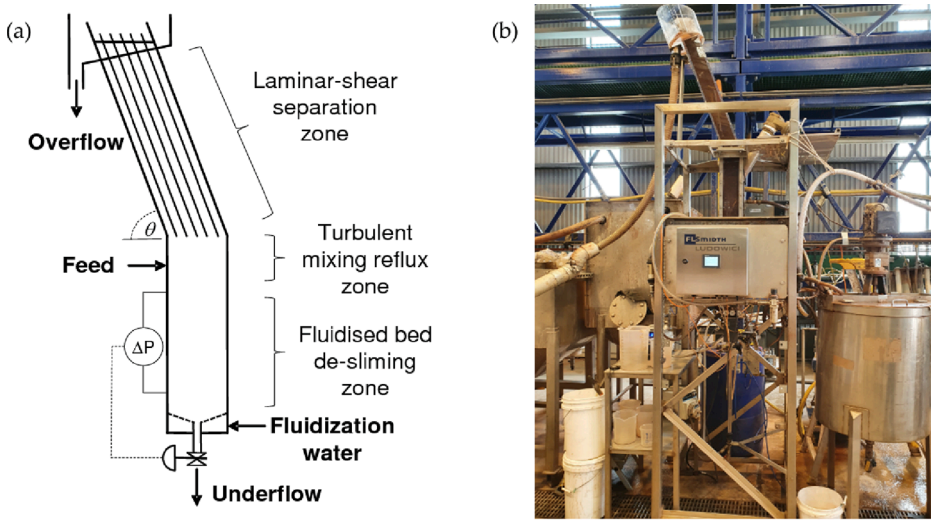

Fig. 4. Reflux Classifier (a) schematic representation (b) image of laboratory system.

Fig. 5. Randomly sorted buckets of the feed slurry prepared prior to an experiment.

Table 3
Summary of conditions used in the experimental program on Sample A.

Run No.	Channel spacing (mm)	Set point (kg/m^3)	Feed rate (L/min)	Throughput (t/m^2/h)	Pulp density (w/w %)	Fluidisation rate (L/min)
1	1.8	2000	2	5	26	0.12
2			6	10	26	0.14
3			4	7	26	
4		2200	5	9	27	
5		2100		9	27	
6		1900		9	27	
7		2000		14	36	
8				6	16	
9				9	27	0.17
10				9	27	0.20
11	3.0			10	27	0.14
12			8	9	16	
13	1.8			9	17	

feed pulp density fixed at 27 % solids (close to the target of 26 %), and the fluidization rate remained at 0.14 L/min. The feed pulp density was then varied in the next two experiments, set at 36 wt% solids and then 16 wt% solids, with the density set point at 2000 kg/m^3. All other settings remained fixed. In the next two experiments the fluidization rate was increased beyond the level deemed ideal, known as the minimum fluidization rate, to 0.17 L/min and then 0.20 L/min, while the feed pulp density returned to 27 wt% solids.

In the next two experiments the inclined channel spacing was increased to 3.0 mm. The density set point was fixed at 2000 kg/m^3 and the fluidization rate set at 0.14 L/min. The first of these experiments used a feed flow rate of 5 L/min, with the feed pulp density set at 27 wt% solids. In the following experiment the feed rate was increased to 8 L/min to produce a higher shear rate. However, the feed pulp density was reduced to 16 wt% solids, a decision based on knowledge acquired during the program of work. In the final experiment the channel spacing was returned to 1.8 mm, however the feed rate was increased to 8 L/min, with the feed pulp density again set at the lower level, this time 17 wt% solids.

The density of the feed particles used in these experiments was measured using pycnometry. The average density across 13 experiments was 3531 kg/m^3 and the standard deviation was 13 kg/m^3, a variation of just 0.4 %.

Finally, it is noted that one additional experiment was conducted on Sample B, adopting virtually the same conditions as those used in Run 2 for Sample A. Here, the fluidization rate used for Sample B was raised to 0.2 L/min due to the denser and hence faster settlings particles.

2.5. Rheology of the slimes

The rheology of the suspension medium was measured using an Anton-Paar MCR102 Rheometer to investigate the above hypothesis that the suspension viscosity increased significantly as the feed pulp density increased. The overflow reject sample from Run 13 was wet screened at 20 μm. The material in the size-range from 0 to 20 μm was then dried, and the density of the particles measured using pycnometry. A series of samples of different pulp density and hence solids volume fraction was prepared, and, for each, the suspension viscosity measured as a function of the shear rate.

3. Results and discussion

3.1. Effect of feed throughput on separation performance

The Reflux Classifier offers a significant throughput advantage over more conventional fluidized bed separators, estimated to be up to 50-fold when targeting the recovery of particles with a density of 4000 kg/m^3 down to a particle size of 10 μm. Galvin (2021) provides the detailed basis behind this estimation. In order to be competitive with the reverse flotation it was necessary to secure a successful separation at a solids throughput of at least 5 t/m^2/h. Thus, the initial series of experiments focussed on the effects of changes in the volumetric flowrate at the fixed feed pulp density of 26 wt% solids, covering a solids throughput range of 5–10 t/m^2/h. The operating conditions involved a fixed lamella channel spacing of 1.8 mm, density set point of 2000 kg/m^3, and fluidization rate of 0.14 L/min (Run 1 was set at 0.12 L/min). The vessel cross-sectional area was always 0.01 m^2.

Table 4 provides a summary of the overall results obtained for the first three experiments. Interestingly, the product grade improved significantly with increases in the volumetric flow rate, reaching an iron grade of 64.6 % in Run 2, however the iron recovery decreased to 73.2 %. Table 5 shows the balanced data set for Run 2 conducted at the highest solids throughput of 10 t/m^2/h. Note the raw data, given in Table 6, are very consistent with the balanced values, confirming the value of the experimental method described earlier. Based on an error

Table 4
Effect of throughput on separation performance.

Run	Feed rate (L/min)	Throughput ($t/m^2/h$)	Feed Grade (%Fe)	(SiO_2)	Product Grade (%Fe)	(SiO_2)	Reject Grade (%Fe)	(SiO_2)	Yield (%)	Iron Recovery (%)
1	2.0	4.7	36.5	44.6	45.1	32.8	16.0	72.9	70.5	87.0
3	4.0	7.3	36.4	44.8	59.7	12.0	14.4	75.8	48.6	79.7
2	6.0	10.0	37.2	43.7	64.6	4.9	17.2	71.9	42.1	73.2

Table 5
Balanced data ser for Run 2 – throughput 10 $t/m^2/h$.

	Feed		Product		Reject	
Sieve size (mm)	**Mass** (%)	**Grade** (%Fe)	**Mass** (%)	**Grade** (%Fe)	**Mass** (%)	**Grade** (%Fe)
0.250	0.4	18.5	0.5	28.7	0.3	5.3
0.180	4.2	17.2	4.0	40.0	4.4	2.1
0.150	6.9	19.4	5.8	51.0	7.8	2.1
0.125	6.6	19.8	4.8	59.3	7.9	2.1
0.090	20.3	25.2	17.1	65.6	22.7	3.0
0.063	16.2	35.0	18.1	68.5	14.9	5.2
0.045	14.2	47.3	20.7	68.8	9.5	13.1
0.038	6.1	52.5	8.9	69.1	4.0	25.3
0.020	10.1	57.4	13.9	68.4	7.3	42.0
−0.020	15.1	48.5	6.2	57.0	21.5	46.7
Overall	**100**	**37.2**	**100**	**64.6**	**100**	**17.2**

Table 6
Raw data set for Run 2 – throughput 10 $t/m^2/h$.

	Feed		Product		Reject	
Sieve size (mm)	**Mass** (%)	**Grade** (%Fe)	**Mass** (%)	**Grade** (%Fe)	**Mass** (%)	**Grade** (%Fe)
0.250	0.3	18.5	0.6	28.8	0.3	5.3
0.180	4.1	17.2	4.0	39.9	4.4	2.1
0.150	6.9	19.4	5.3	51.0	8.1	2.1
0.125	6.3	19.8	4.8	59.2	7.6	2.1
0.090	21.1	25.3	13.3	65.2	25.7	3.0
0.063	16.6	34.9	19.9	68.5	13.1	5.2
0.045	13.7	47.3	21.5	68.8	9.0	13.1
0.038	5.7	52.5	9.6	69.1	3.9	25.3
0.020	9.8	57.0	15.0	68.7	6.8	42.1
−0.020	15.5	48.7	6.1	56.8	21.2	46.6
Overall	**100**	**36.9**	**100**	**65.3**	**100**	**17.2**

analysis at the end of this paper, it is estimated the uncertainty in the grade and recovery are both +/−0.4 %. There is strong confidence therefore in the reliability of this key result.

Fig. 6 shows the iron and silica grades in the underflow product stream as a function of the particle size. Although the iron grade declines significantly at particle sizes larger than about 100 μm, there is relatively little solids in the coarser size fractions, hence the overall grade remains high. The silica grade is initially very low, but climbs significantly beyond a particle size of 100 μm.

The partitioning of the silica to the underflow product is shown as a function of the particle size in Fig. 7. These data show the very strong effect of the feed flow rate and hence solids throughput on the probability of the coarser silica particles reporting to the underflow product. At the highest feed flow rate, the partition numbers are significantly lower, making the iron grade of the product significantly higher. This finding is consistent with the mechanism of a shear induced inertial lift force within the inclined channels that causes the coarse silica to physically lift from the upward facing surfaces and in turn convey to the overflow.

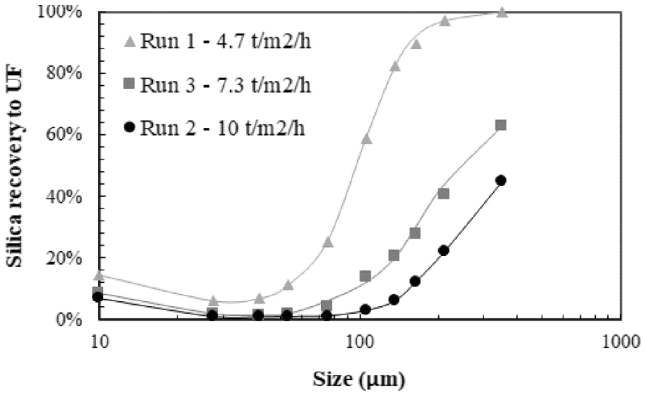

Fig. 7. Effect of the throughput on the silica partition to the underflow (UF) product. It is evident the highest throughput leads to the lowest partitioning of the silica to the product.

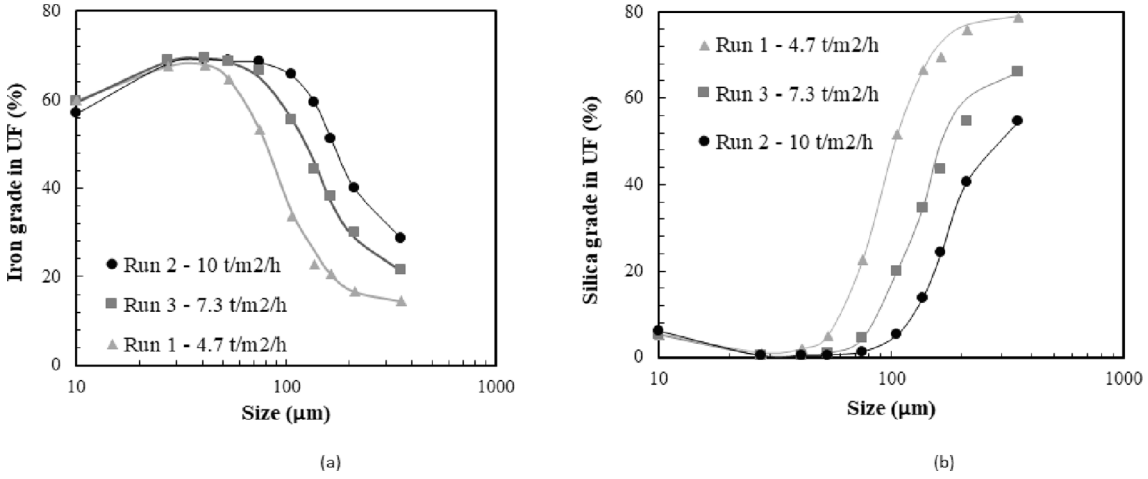

Fig. 6. Effect of throughput on separation performance - iron (a) and silica (b) grades versus particle size in the underflow (UF) product.

3.2. Effect of bed density set point

For a given set of operating conditions, the primary control variable is the density set point. The interpretation of the measured signal is important. Here pressure transducers were located at elevations above the fluidization distributor of 60 and 440 mm as shown in Fig. 4A. The transducers measure the weight loading of the suspension above each probe, hence the difference is the weight loading of the suspension between the probes. If there is a distinct fluidized bed level located between the probes, then part of the reading will relate to the low concentration zone above the bed and the rest to the suspension within the bed. Solids that are supported mechanically off the base of the vessel and not by the fluid are not recognised by the pressure transducers. So, the bed must be sufficiently fluidized for the reading to have meaning, a condition which is therefore essential to the control of the system.

For a well liberated feed, the suspension density is arguably just a measure of the height of the fluidized bed when the bed level is located between the elevation of the probes. The extent to which the bed density can be increased is governed by the level of coarse silica that ends up in the bed. If the silica content is excessive, then it becomes difficult to reach a high suspension density. In this case the bed level will tend to increase, limiting the underflow discharge to achieve the set point. In general, a lower density set point promotes a higher yield to underflow, hence a higher recovery, but a lower grade.

Table 7 summarizes the results obtained using the three density set points ranging from 2200 kg/m^3 down to 1900 kg/m^3. These experiments used a fixed inclined channel spacing of 1.8 mm, keeping the feed rate fixed at 5 L/min, the pulp density at 27 wt% solids, and the fluidization rate at 0.14 L/min. The feed solids throughput was 9 t/m^2/h. At this stage of the work, the benefits of a higher volumetric feed rate of 6 L/min were not known.

Run 4, operated at a set point of 2200 kg/m^3, produced the highest product grade of 60.7 % and lowest iron recovery of 67.8 %. This result is therefore compared with the findings from Run 2 which previously had the highest product grade of iron of 64.6 % at an iron recovery of 73.2 %. The significantly higher set point used here of 2200 kg/m^3 has likely resulted in the lower iron recovery, restricting the underflow discharge to target the high bed density set point. In fact, the average iron recovery produced for set points of 1900 and 2100 kg/m^3 (75.6 %, 70.7 %) is close to the result obtained for Run 2 (73.2 %) operated at the intermediate density set point of 2000 kg/m^3.

Interestingly the highest iron grade of 60.7 % is significantly lower than the grade of 64.6 % obtained in Run 2 despite the use of a significantly higher set point density in Run 4. Runs 4–6 involved a volumetric feed rate of 5 L/min. Run 2 involved the higher volumetric feed rate of 6 L/min. At this stage of the experimental program, it was not apparent that this modest increase in the volumetric feed rate to 6 L/min was important, hence most of the work continued at the lower feed rate of 5 L/min. While it is possible a statistical design might have identified the optimal separation with fewer experiments, the systematic series of experiments offered strong clarity relating cause and effect.

The shear induced inertial lift is higher at 6 L/min than for the experiments conducted at lower volumetric feed rates. Physical lift is a critical phenomenon (Galvin and Liu, 2011; King and Leighton, 1997). Once the lift force exceeds the net weight of the particle in the fluid, in the normal direction to the incline, physical lift occurs. But no lift occurs if the lift force does not reach this level. When physical lift occurs, the particles migrate to more central positions within the inclined channels where the local fluid velocities are substantially higher. These particles then convey upwards as part of the overflow reject stream. In this series of experiments the feed flow rate of 5 L/min was not sufficient to convey some of the coarse particles hence the product grades decreased significantly in comparison to Run 2 which had a feed flow rate of 6 L/min.

Fig. 8 shows the partitioning of the iron to the underflow product as a function of the particle size. The results obtained at the two lowest density set points of 1900 and 2100 kg/m^3 are indicative of the Run 2 recoveries obtained using the intermediate density set point of 2000 kg/m^3, which involved a higher feed flow rate of 6 L/min. Fig. 9 compares the size partition curves for the silica from Run 2 at 2000 kg/m^3 and 10 t/m^2/h with the experiment here at a set point of 2200 kg/m^3 and 9 t/m^2/h. As noted, the former experiment achieved an iron grade of 64.6 % and the latter 60.7 %. These results appear to confirm the importance of the hydrodynamics in the inclined channels, and that the slightly higher volumetric flow rate conveys the coarse silica to the overflow reject stream, thus increasing the iron grade in the underflow product stream.

3.3. Effect of fluidization water rate

The fluidization rate must be set at a level sufficient to support the weight of the particles within the fluidized bed. This requirement is essential simply from a process control perspective, to ensure the physical state of the steady state system is characterised uniquely by the measured suspension density. It is also important to ensure the bed can act as a zone for sorting particles, permitting the upwards displacement of the relatively low-density particles from the bed, the so-called inversion phenomenon reported by previous researchers (Moritomi et al., 1982; Moritomi et al., 1986). The quiescent nature of the fluidized bed acts as a buffer, permitting ultrafine low-grade slimes to permeate out of the bed, improving product grade and subsequent dewatering. The fluidization rate was first set at 0.12 L/min, but later shifted to 0.14 L/min.

This section considers the effects of utilising an excessive fluidization rate on separation performance. This work involved a fixed lamella channel spacing of 1.8 mm, bed density set point of 2000 kg/m^3, volumetric feed rate of 5 L/min, and feed pulp density of 27 wt% solids. The solids throughput was again 9 t/m^2/h. The use of excessive fluidization water causes an expansion of the bed to lower concentrations, and hence the need for the bed height to increase when targeting the density set point. This bed expansion can invite coarse silica to join the bed, leading to poorer product grade. The most significant effect, however, is the loss of ultrafine particles of hematite. While these may well be captured by the inclined channels, and hence returned to the lower zone, the high fluidization rate ultimately creates a barrier to their transport into the underflow product stream. Table 8 shows that as the fluidization rate increases the iron recovery decreases. In Run 2 the iron recovery (at a higher feed rate of 6 L/min) was 73.2 %. Here the recovery decreased to 71.4 % for a fluidization rate of 0.17 L/min, and to 66.8 % at a fluidization rate of 0.20 L/min.

Table 7
Effect of bed density set point on separation performance.

Run	Set Point (kg/m^3)	Feed Grade		Product Grade		Reject Grade		Yield	Iron Recovery
		(%Fe)	(%SiO_2)	(%Fe)	(%SiO_2)	(%Fe)	(%SiO_2)	(%)	(%)
4	2200	36.0	44.3	60.7	11.9	19.3	66.0	40.1	67.8
5	2100	36.9	43.7	60.4	12.6	19.0	67.4	43.2	70.7
6	1900	36.3	43.9	58.1	14.3	16.8	70.3	47.2	75.6

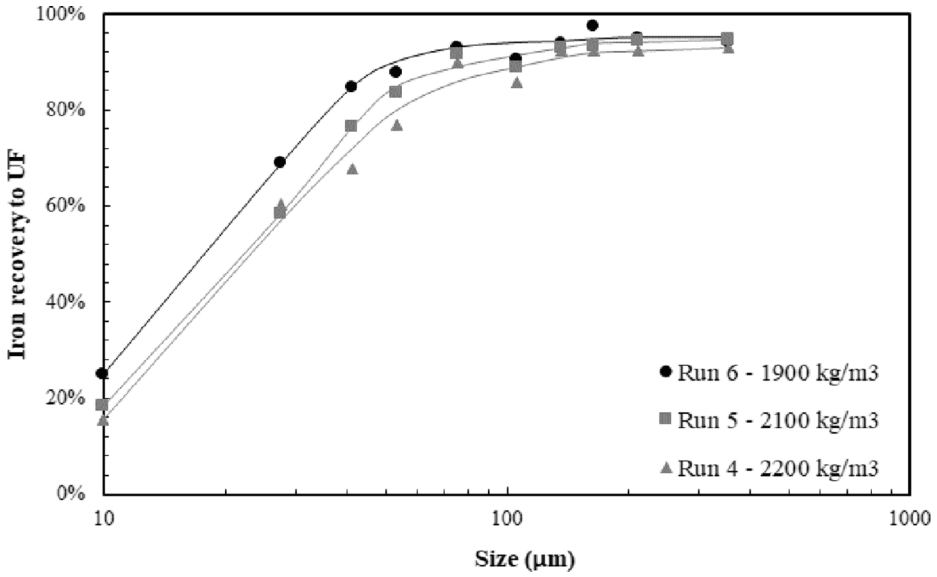

Fig. 8. Effect of bed density set point on the iron partition to the underflow (UF) product.

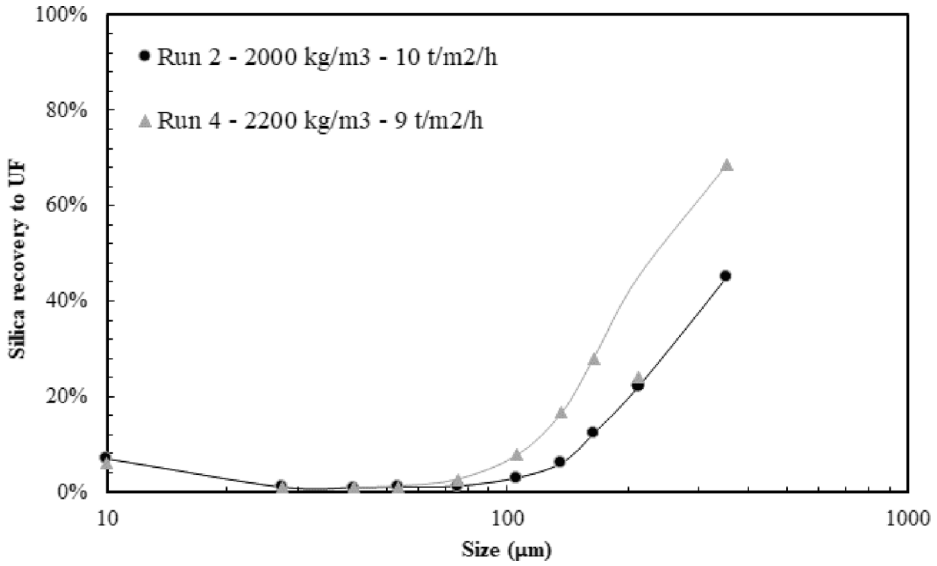

Fig. 9. Effects of bed density set point and feed throughput on the silica partition to the underflow (UF) product. The higher volumetric rate of Run 2 (6 L/min) compared to Run 4 (5 L/min) led to less silica recovery in the underflow.

Table 8
Effect of fluidization rate on the separation performance.

Run	Fluidization water rate	Feed Grade		Product Grade		Reject Grade		Yield	Iron Recovery
	(L/min)	(%Fe)	(SiO_2)	(%Fe)	(SiO_2)	(%Fe)	(SiO_2)	(%)	(%)
9	0.17	37.3	43.6	61.3	9.7	18.8	69.6	43.4	71.4
10	0.20	37.1	43.8	61.4	9.6	20.7	67.0	40.4	66.8

Table 9
Effect of feed pulp density on separation performance.

Run	Pulp Density	Throughput	Feed Grade		Product Grade		Reject Grade		Yield	Iron Recovery
	(w/w %)	($t/m^2/h$)	(%Fe)	(SiO_2)	(%Fe)	(SiO_2)	(%Fe)	(SiO_2)	(%)	(%)
7	36	14	36.8	44.2	61.2	9.8	26.8	58.3	29.0	48.2
8	16	6	35.5	46.1	54.3	19.7	14.3	75.9	53.1	81.0

3.4. Effect of the feed pulp density on separation performance

The feed pulp density used in this study was set at the nominal level expected in the industrial setting, at about 26 to 27 wt% solids. For a given volumetric feed rate, it is in principle possible to achieve a much higher solids throughput, with acceptable recovery, by increasing the feed pulp density. Thus, the first of these experiments involved the higher feed pulp density of 36 %. The conditions of the experiments listed in Table 9 involved a channel spacing of 1.8 mm, set point 2000 kg/m^3, volumetric feed rate of 5 L/min, and fluidization rate of 0.14 L/min. It is evident that the iron recovery achieved using the high feed pulp density of 36 % was very low at 48.2 %. The conclusion drawn from this work is that the viscosity of the feed suspension increases with the feed pulp density. In previous work, Carpenter et al (2019) undertook a systematic study on the effects of suspension viscosity, showing the considerable impact on particle recovery. In that work significantly higher recoveries were achieved by halving the feed pulp density while doubling the volumetric feed rate.

In order to investigate the effect of viscosity further, Run 8 was conducted at the lower feed pulp density of 16 %, producing a very high iron recovery of 81 %. This case indicates a pulp density of 16 % is almost sufficient to "switch off" the effects of elevated viscosity. This issue is examined later through direct measurement of the suspension viscosity at different concentrations. Interestingly, the product grade decreased significantly to 54.3 %. This result suggests the silica partitioning to the underflow increased because of the reduction in the suspension viscosity. Moreover, the result suggested there could be significant benefits from increasing the volumetric feed rate to improve the shear induced inertial lift, while also increasing the solids throughput, and most importantly improving the product grade.

3.5. Effect of increasing the volumetric feed rate at low feed pulp density

The initial three experiments conducted in this study showed the profound effect of increasing the volumetric feed rate from 2 to 4 to 6 L/min. The separation performance improved as the volumetric feed rate increased. Subsequent work conducted at 5 L/min consistently produced a performance below that observed at 6 L/min. The iron grades at the lower volumetric feed rate of 5 L/min never reached 62 %, but at 6 L/min the grade reached 64.6 %. A second key observation in this work is that a reduction in the feed pulp density leads to improved performance, most likely due to the reduction in the suspension viscosity. In this section experiments were conducted using a volumetric feed rate of 8 L/min, with the feed pulp density reduced to 16–17 wt% solids. In both cases the solids throughput was 9 t/m^2/h. The density set point was set at 2000 kg/m^3, and fluidization rate at 0.14 L/min. The first of these experiments was conducted using an inclined channel spacing of 3.0 mm. The iron grade increased to 65.1 %, the highest so far in the study, and the iron recovery reached 71.7 %. In the next experiment the inclined channel spacing was reduced to 1.8 mm. This experiment produced the best overall performance from the study, an iron grade of 65.6 % and iron recovery of 72.9 %. These grades were better than that from Run 2 (lower grade of 64.6 %, recovery marginally higher at 73.2 %).

These research findings reveal a robust scenario where a viscosity problem can be addressed by reducing the feed pulp density while increasing the volumetric feed rate to compensate for any loss in the solids throughput. The primary limitation in securing a higher-grade product is the tendency for the coarse silica to partition to the underflow product.

3.6. Effect of the inclined channel spacing

In this section the performance of the Reflux Classifier operated with a channel spacing of 3.0 mm, with the feed flow rate reduced to the standard 5 L/min, was investigated. Here the feed pulp density was set at the usual 27 wt% solids, density set point at 2000 kg/m^3, and fluidization rate at 0.14 L/min. Table 10 provides a summary of the results. The conditions led to a lower iron recovery of 65.7 % due to the reduction in the capture efficiency of the ultrafine particles due to the wider channels. The return to the higher feed pulp density and hence suspension viscosity also impacted negatively on the iron recovery. However, the product grade reached a level of 63.6 %. This was surprising given the shear rate within the inclined channels would have been lower due to the 3.0 mm wide channel spacing and the lower volumetric feed rate of 5 L/min. The higher suspension viscosity associated with the feed pulp density of 27 % probably assisted with the inertial lift, and in turn the conveying of the coarse silica up through the inclined channels.

It is worth noting that the performance of the Reflux Classifier with the wider channel spacing of 3.0 mm was relatively close to that observed for the channel spacing of 1.8 mm in Run 2. If the level of coarse silica could be reduced, the wider channel system would prove highly effective in beneficiating the itabirite resource.

3.7. Reflux classifier experiment on Sample B

Table 11 presents the test conditions used for Sample B. The experimental conditions selected for this experiment were virtually the same as those used in Run 2 for Sample A. Sample B permitted the use of a higher fluidization rate, with less sensitivity to losses, probably due to the higher proportion of hematite. Sample A was clearly more sensitive to a higher fluidization rate, perhaps due to the significant presence of the goethite. Table 12 provides a summary of the results following mass balance reconciliation showing a remarkably high iron grade of 66.3 % and high iron recovery of 84.7 %.

The experimental results produced for Sample B are best compared with those obtained in Run 2 for sample A. Firstly the product grade for Sample A was 64.6 % and for Sample B 66.3 % while the recoveries were 73.2 % and 84.7 % respectively. Sample A has a significant level of goethite (mineral density ~ 4.3 t/m^3), and 45 % hematite (mineral density up to 5.3 t/m^3) as shown in Table 2. Sample B had only 1 % goethite, and 57 % hematite. It is probable that the high proportion of

Table 11
Experimental conditions used for Sample B.

Channel spacing (mm)	Set Point (kg/m^3)	Fluidization (L/min)	Throughput (t/m^2/h)	Flow Rate (L/min)	Pulp Density (%)
1.8	2000	0.2	10	6	24

Table 10
Effects of channel spacing on separation performance.

Run	Pulp Density (wt %)	Channel Spacing (mm)	FlowRate (L/min)	Throughput (t/m^2/h)	Product Grade		Reject Grade		Yield (%)	Iron Recovery (%)
					(%Fe)	(%SiO_2)	(%Fe)	(%SiO_2)		
2	26	1.8	6	10	64.6	4.9	17.2	71.9	42.1	73.2
11	27	3.0	5	10	63.6	6.6	19.9	67.6	37.5	65.7
12	16	3.0	8	9	65.1	4.5	17.3	71.4	40.1	71.7
13	17	1.8	8	9	65.6	3.8	17.0	73.1	41.1	72.9

Table 12
Summary of experimental results obtained for sample B.

Feed Grade		Product Grade		Reject Grade		Yield	Iron Recovery
(%Fe)	(% SiO_2)	(% Fe)	(% SiO_2)	(% Fe)	(% SiO_2)	(%)	(%)
41.4	39.0	66.3	4.4	13.4	77.7	52.9	84.7

hematite in Sample B led to the stronger iron recovery especially at the finer sizes as shown in Fig. 10. Interestingly, Fig. 10 also shows the partition of the silica to the underflow product was almost the same for the two experiments.

Fig. 11 shows the particle size distribution of the feed, product and reject from the experiment conducted on Sample B. The overflow reject is much coarser than the underflow product, showing the Reflux Classifier was very efficient in removing the coarse quartz contained in the feed (Table 1). However, it is also evident there are losses of ultrafines in the overflow containing iron, something that is inevitable in gravity separation. Table 13 shows the balanced data set for the Sample B separation showing the losses of ultrafine iron in the overflow. The raw data set is shown in Table 14.

Table 13
Balanced data set for Sample B separation.

Sieve size	Feed		Product		Reject	
	Mass	Grade	Mass	Grade	Mass	Grade
(mm)	(%)	(%Fe)	(%)	(%Fe)	(%)	(%Fe)
0.25	1.3	1.4	1.4	1.8	1.3	1.0
0.18	4.1	2.4	1.8	6.0	6.7	1.2
0.15	4.9	4.7	1.0	31.3	9.3	1.5
0.13	4.3	8.9	1.1	52.4	7.9	2.0
0.09	14.3	20.6	8.0	64.8	21.4	2.1
0.06	19.1	45.5	23.6	69.1	14.1	1.4
0.05	18.0	57.7	28.1	69.5	6.7	2.0
0.04	5.1	59.2	8.1	69.5	1.7	3.4
0.02	12.4	60.1	19.5	69.6	4.4	12.2
−0.02	16.4	49.7	7.4	68.1	26.5	44.0
Overall	**100.0**	**41.4**	**100.0**	**66.3**	**100.0**	**13.4**

3.8. Rheology of the slimes

Shear rates of 6U/z are produced at the planar surface of the inclined channels, where U is the channel superficial velocity based on the overflow rate, and z the channel spacing (Galvin and Liu, 2011). The shear rates within the inclined channels were calculated and used to guide the selection of the conditions in the rheometer. The suspension viscosities were therefore determined as a function of the solids

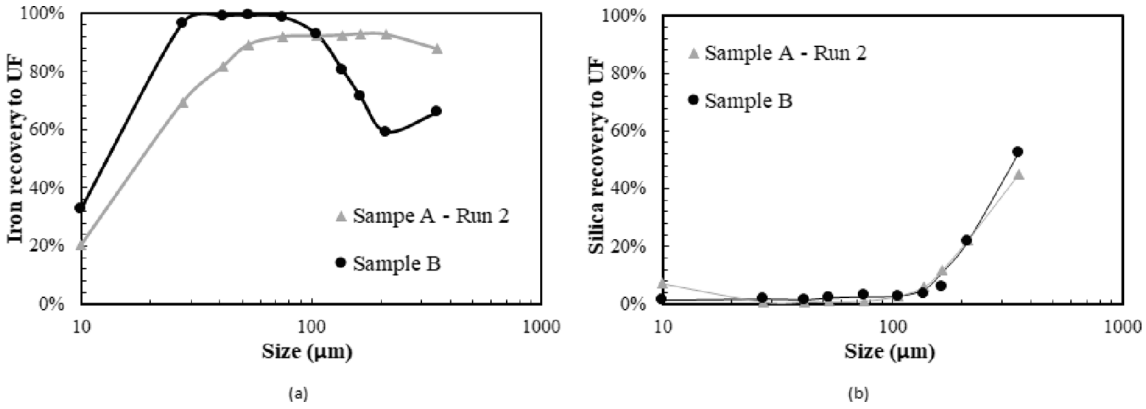

Fig. 10. Comparison between Sample A-Run 2 and the Sample B separation. (a) Iron recovery versus particle size and (b) partition of silica to the underflow product versus particle size.

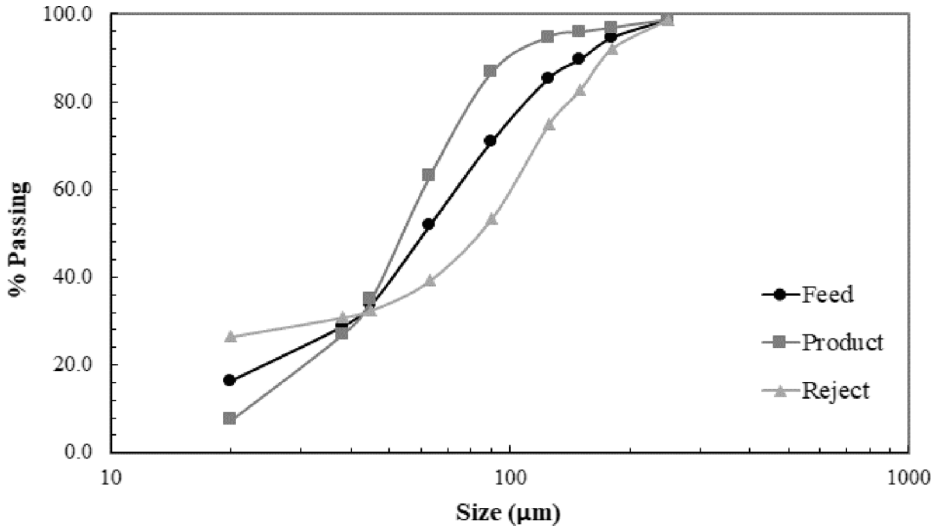

Fig. 11. Particle size distributions of the feed, product, and reject streams for the Sample B separation.

Table 14
Raw data set for Sample B separation.

Sieve size	Feed		Product		Reject	
	Mass	Grade	Mass	Grade	Mass	Grade
(mm)	(%)	(%Fe)	(%)	(%Fe)	(%)	(%Fe)
0.25	1.4	1.5	1.3	1.7	1.3	1.0
0.18	4.5	2.4	1.5	6.0	6.7	1.2
0.15	5.2	4.7	0.8	31.2	9.5	1.5
0.13	4.2	8.9	0.9	52.2	8.8	2.0
0.09	12.8	20.7	6.5	64.6	21.1	2.1
0.06	20.0	45.8	20.9	69.0	13.0	1.4
0.05	17.0	57.8	31.1	69.7	6.3	2.0
0.04	5.3	59.0	8.5	70.0	1.5	3.4
0.02	12.1	60.1	21.2	69.8	4.2	12.2
−0.02	17.5	50.0	7.2	68.1	27.5	44.1
Overall	**100.0**	**39.9**	**100.0**	**67.1**	**100.0**	**13.4**

concentration at specific shear rates of 33 s^{-1} (based on Run 12 with 3 mm channels), 45 s^{-1} (based on Run 2), and 63 s^{-1} (based on Run 13).

Fig. 12 shows the slimes viscosity on a log scale as a function of the solids volume fraction across a broad range of concentration for the three shear rates. The strong exponential relationship is clear. Fig. 13 presents the same data in a more relevant form, with the slimes viscosity on a linear scale as a function of the pulp density, covering the smaller range of concentration used in this work. Run 7 had a feed pulp density of 36 wt% solids and overflow pulp density of 29 wt% solids thus the viscosity of the suspension likely exceeded 9 mPas. Run 2 had a feed pulp density of 26 wt% solids and overflow pulp density of 17 wt% solids thus the viscosity was much lower, and likely exceeded 2 mPas. Run 13 had a feed pulp density of 17 wt% solids and overflow pulp density of 11 % solids thus the viscosity likely exceeded about 1 mPas, the viscosity of water. These data show the effects of the suspension viscosity were largely eliminated by reducing the feed pulp density down to ~ 17 wt% solids. The data also helps to explain the poor iron recovery in Run 7 at the highest feed pulp density of 36 wt% solids.

3.9. Error analysis

The direct comparison of the balanced and raw data sets reveals very strong steady state consistency, and in turn very low mass balance errors across this work. The average error in the assays between Table 5 and Table 6 and between Table 13 and Table 14 is 0.6 % of the assay value, neglecting outliers including errors of zero. Thus, the highest grades in this work were 65.6+/−0.4 % for Sample A and 66.3+/−0.4 % for Sample B. Using this uncertainty in the assays, and the two product

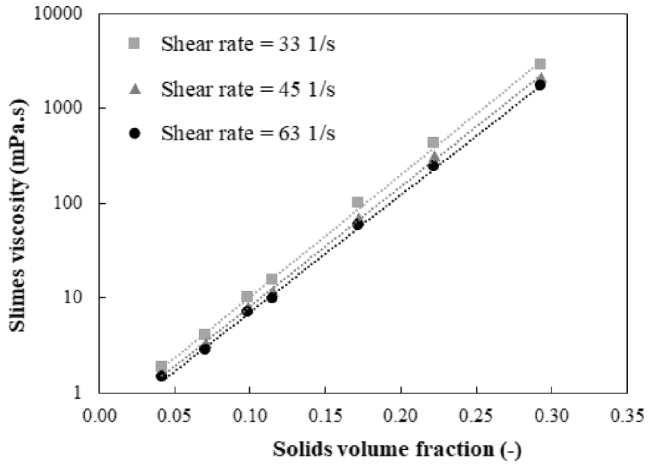

Fig. 12. The viscosity of the suspension containing the slimes shown as a function of the solids volume fraction, with a clear exponential dependence on the concentration.

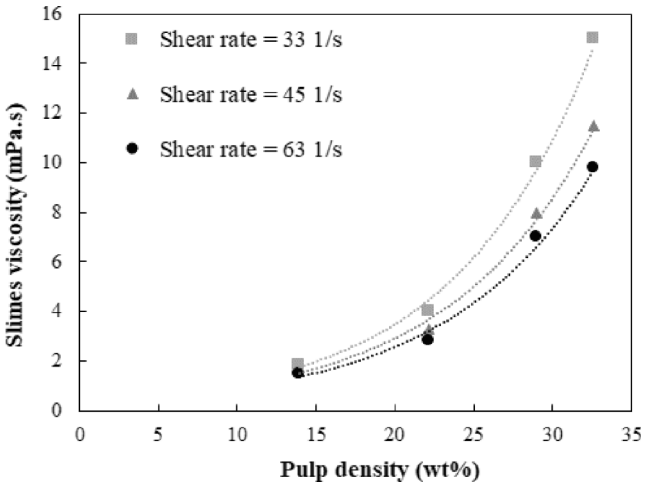

Fig. 13. Slimes viscosity of the 0–20 μm particles as a function of the pulp density for three shear rates.

formulae for recovery, a Monte Carlo analysis produced an estimated error in the recovery of 0.6 % of the recovery value. Thus, the corresponding recoveries for Samples A and B were 72.9+/−0.4 % and 84.7+/−0.5 % respectively. As noted previously, this precision is attributed to the experimental method used to deliver the feed.

This research involved a systematic program of experiments aimed at developing an understanding of the underlying, albeit complex, physical processes involved in the hydrodynamic transport of the particles through the Reflux Classifier. Highly consistent data sets were generated, ideal for validating future models. Part II of this study uses the data set to assess the extent to which the data conform to a generic partition surface. It is evident the feed is largely of a binary nature, meaning the separation performance could be assessed using the partition surface covering the low-density quartz and the high-density hematite, modified slightly to reflect the mineralogy. By using this data set to validate the partition surface it will be possible for practitioners to readily predict the potential grade-recovery relationship for very different feeds.

4. Conclusions

This paper provides a comprehensive and detailed investigation of the gravity separation of a dense mineral feed in a Reflux Classifier. The experimental conditions covered different density set points, feed pulp densities, throughputs, fluidization water rates and lamella channel spacings. The work showed the clear potential of a single stage gravity separator in upgrading dense minerals down towards a lower nominal particle size of 10 μm. This means that gravity separation could be used to replace reverse flotation, resulting in a significant reduction in the complexity, cost, and environmental impact of the beneficiation circuit. Although the bed density set point provides an effective measure of control, other factors are arguably more important, especially those that impact on the hydrodynamics within the inclined channels.

The feed iron grade was upgraded from 37 % to 65.6 % at a recovery of 72.9 %. Note that pure hematite has an iron grade of 69.9 %. The loss in recovery is attributed to the slow settling of the relatively fine particles and to the presence of goethite in the iron ore. The solids throughput achieved was 9 $t/m^2/h$, notably higher than achieved by reverse flotation (typically 4 $t/m^2/h$). A separate feed, Sample B, containing much less goethite, was also processed in the Reflux Classifier, achieving an iron grade of 66.3 % and iron recovery of 84.7 %. This work demonstrated the importance of maintaining a sufficient volumetric feed rate to promote shear induced inertial lift of the coarse gangue silica within the inclined channels. These conditions are needed to convey these particles into the overflow reject stream. Interestingly, the separation performance improved as the throughput was increased.

Benefits were also observed by reducing the feed pulp density, most likely due to the corresponding reduction in the suspension viscosity. In fact, the poorest performance was obtained at a higher feed pulp density of 36 wt% while the best performance was observed at the lower feed pulp density of ~ 17 wt%. The best overall results were obtained by increasing the volumetric feed rate to 8 L/min and lowering the feed pulp density to 17 wt% solids.

The fluidization rate must be set at a rate sufficient to suspend the particles in the lower bed. This work showed that excessive fluidization caused a strong decline in the iron recovery. Finally, although most of this work involved an inclined channel spacing of 1.8 mm, and it was concluded that this spacing gave the best performance, the separations observed using a channel spacing of 3.0 mm were more than satisfactory. Moreover, any reduction in the level of coarse silica in the feed would deliver a step change improvement in product grade.

Declaration

The authors acknowledge the University of Newcastle has a Research and Development Agreement with FLSmidth, and IP policy that extends benefits to the inventor, Kevin Galvin.

CRediT authorship contribution statement

Armando F.d.V. Rodrigues: Conceptualization, Methodology, Investigation, Writing – original draft, Writing – review & editing, Formal analysis, Funding acquisition. **Homero Delboni Junior:** Supervision, Writing – review & editing, Formal analysis. **Otavia M.S. Rodrigues:** Writing – review & editing, Formal analysis. **James Zhou:** Methodology, Investigation, Writing – review & editing, Formal analysis. **Kevin P. Galvin:** Conceptualization, Investigation, Writing – original draft, Writing – review & editing, Formal analysis, Supervision, Funding acquisition.

Declaration of Competing Interest

The authors declare the following financial interests/personal relationships which may be considered as potential competing interests: Kevin Galvin reports financial support was provided by Australian Research Council. Kevin Galvin reports research funding from Vale. Kevin Galvin reports financial support and equipment were provided by FLSmidth. Kevin Galvin reports a relationship with FLSmidth that includes: funding grants. Kevin Galvin has patent issued via his employer to Licensee. Kevin Galvin, Associate Editor, Minerals Engineering.

Data availability

The most relevant data is already included in the paper.

Acknowledgements

The authors would like to thank Vale S.A. for sponsoring the work as well as providing permission to publish the work.

The authors also acknowledge the funding support from the Australian Research Council for the ARC Centre of Excellence for Enabling Eco-Efficient Beneficiation of Minerals, grant number CE200100009, and other research support from FLSmidth.

Appendix A. Supplementary material

Supplementary data to this article can be found online at https://doi.org/10.1016/j.mineng.2023.108187.

References

Amariei, D., Michaud, D., Paquet, G., Linday, M., 2014. The Use of the Reflux Classifier for Iron Ores: Assessment of Fine Particles Recovery at Pilot Scale. Miner. Eng. 62, 66–73.

Carpenter, J.L., Zhou, J., Iveson, S.M., Galvin, K.P., 2019. Gravity Separation in the REFLUX™ Classifier in the Presence of Slimes. Miner. Eng. 143, 105941.

Crompton, L.J., Islam, M.T., Galvin, K.P., 2022. Investigation of Internal Classification in Coarse Particle Flotation of Chalcopyrite Using the CoarseAIR™. Minerals 12, 783.

Dai. Z., Fornaziero, D., Ralston, J., 2000. Particle-bubble collision models – a review. In: Advances in Colloid and Interface Science, 85(2-3), 231-256.doi.org/10.1016/S0001-8686(99)00030-5.

Filippov, L.O., Severov, V., Filippova, I.V., 2014. An overview of the beneficiation of iron ores via reverse cationic flotation. Int. J. Miner. Process 127, 62–69. https://doi.org/10.1016/j.minpro.2014.01.002.

Filippov, L.O., Silva, K., Piçarra, A., Lima, N., Santos, I., Bicalho IV, L., Filippova, P.A., 2021. Iron Ore Slimes Flotation Tests Using Column and Amidoamine Collector without Depressant. Minerals 11 (7), 699.

Fornasiero, D., Filippov, L.O., 2017. Innovations in the flotation of fine and coarse particles. J. Phys. Conf. Ser. 879, 012002 https://doi.org/10.1088/1742-6596/879/1/012002.

França, J.R.O., Barrios, G.K.P., Turrer, H.D.G., Tavares, L.M., 2020. Comminution and liberation response of iron ore types in a low-grade deposit. Miner. Eng. 158, 106590 https://doi.org/10.1016/j.mineng.2020.106590.

Galvin, K.P., 2021. Process Intensification in the Separation of Fine Minerals. Chem. Eng. Sci. 231, 116293.

Galvin, K.P., Liu, H., 2011. Role of Inertial Lift in Elutriating Particles According to their Density. Chem. Eng. Sci. 66, 3686–3691.

Galvin, K.P., Compton, T., Firth, B.A., 1995. Quantification of the data improvement produced by optimised metallurgical plant mass balances. Miner. Eng. 8 (7), 739–752. https://doi.org/10.1016/0892-6875(95)00036-P.

Galvin, K.P., Iveson, S., 2022. New Challenges for Gravity Concentration and Classification of Fine Particles. Miner. Eng. 190, 107888.

Hagemann, S.G., Angerer, T., Duuring, P., ., C.A, Rosi'ere, Silva, R.C.F., Lobato, L., Hensler, A.S., Walde, D.H.G., 2016. BIF-hosted iron mineral system: a review. Ore Geol. Rev. 76, 317–359.

Holappa, L., 2020. A General Vision for Reduction of Energy Consumption and CO2 Emissions from the Steel Industry. Metals 10 (9), 1117. https://doi.org/10.3390/met10091117.

King, M.R., Leighton, D.T., 1997. Measurement of the inertial lift on a moving sphere in contact with a plane wall in shear flow. Phys. Fluids 9 (5), 1248–1255.

Lima, N.P., Peres, A.E.C., Marques, M.L.S., 2012. Effect of Slimes on Iron Ores Flotation. Int. J. Min. Eng. Miner. Process 1, 43–46.

Lima, N.P., Silva, K., Souza, T., Filippov, L., 2020. The characteristics of iron ore slimes and their influence on the flotation process. Minerals 10 (8), 675. https://doi.org/10.3390/min10080675.

Moritomi, H., Iwase, T., Chiba, T., 1982. A comprehensive interpretation of solid layer inversion in liquid fluidized beds. *Chem. Engng Sci.* 37 (12), 1751Ð1757.

Moritomi, H., Yamagishi, T., Chiba, T., 1986. Prediction of complete mixing of liquid-fluidized binary solid particles. *Chem. Engng Sci.* 41 (2), 297Ð305.

Rodrigues, A.F.V., 2014. Grinding of Itabirite Iron Ore in Autogenous and Semi-Autogenous Mills. University of Queensland. Australia. MPhil thesis.

Segura-Salazar, J., de S.L. Santos, N., Tavares, L.M., 2021, Holistic Pre-Feasibility Study of Comminution Routes for a Brazilian Itabirite Ore, Minerals, 11(8), 894. DOI: 10.3390/min11080894.

Starrett, J., Galvin, K.P., 2023. Application of Inclined Channels in the Hydrodynamic Classification of Minerals by Particle Size. Minerals Engineering 195, 108002.